Available online at www.sciencedirect.com
SCIENCE DIRECT
Cement and Concrete Research 36 (2006) 91 – 98
Cement and Concrete Research

Uptake of Se(IV/VI) oxyanions by hardened cement paste and cement minerals: An X-ray absorption spectroscopy study

Isabelle Bonhoure [a], Isabel Baur [b], Erich Wieland [a,*], C. Annette Johnson [b], André M. Scheidegger [a]

[a] Laboratory for Waste Management, Nuclear Energy and Safety Department, Paul Scherrer Institute, 5232 Villigen, Switzerland
[b] Swiss Federal Institute for Environmental Science and Technology (EAWAG), 8600 Dübendorf, Switzerland

Received 11 August 2004; accepted 3 May 2005

Abstract

The uptake of selenate ($Se^{VI}O_4^{2-}$) or selenite ($Se^{IV}O_3^{2-}$) by hardened cement paste (HCP) and important constituents of the cement matrix such as calcium silicate hydrate (C–S–H), portlandite (CH), ettringite (AFt) and monosulfate (AFm) was investigated using X-ray absorption spectroscopy (XAS). The XAS measurements were conducted on samples with Se loadings ranging between 1200 and 8800 ppm. X-ray absorption near edge structure (XANES) spectroscopy shows that redox reactions do not influence uptake processes in the cementitious systems. The EXAFS (extended X-ray absorption fine structure) spectra of Se(IV) and Se(VI) bound to CH, AFt, AFm and C–S–H are similar to those of SeO_4^{2-} and SeO_3^{2-} in solution, indicating a "solution-like" coordination environment upon uptake by the cement minerals. Similarly, the spectra of Se(IV)- and Se(VI)-treated HCP samples reveal the absence of backscattering atoms at short distances. These results suggest that the coordination sphere of the SeO_4^{2-} and SeO_3^{2-} entities is maintained upon immobilization by HCP and cement minerals and non-specific interactions dominate at the given Se loadings.

Keywords: Cement paste; X-ray absorption spectroscopy; Adsorption; Selenium; Radioactive waste

1. Introduction

Cement is commonly used worldwide to condition radioactive and non-nuclear hazardous waste materials and to construct the engineered barriers in repositories for radioactive waste. The wide variety of mineral structures available in the cement matrix that may accommodate ions from the waste matrices is ideal for the immobilization of many heavy metals and metalloid species. The mobility of selenium in various types of wastes makes it of particular concern to environmental aspects of waste management. Se is often found in high concentrations in leachates due to its enhanced mobility in alkaline media. For example, high Se concentrations (>0.1 mg/L) were determined in water leaving the coal ash disposal pond of coal-fired power plants and coal mines [1,2], whereas lower Se concentrations (<0.1 mg/L) were found in leachates from municipal waste incineration (MSWI) air pollution control (APC) residuals [3]. In radioactive wastes, the fission product ^{79}Se ($t_{1/2} \sim 7 \cdot 10^4$ years) may significantly contribute to the dose curve of radionuclides released from the cementitious near field of a repository [4].

Under typical conditions prevailing in cementitious systems (pH=12–14, -400 mV$<E_h<+200$ mV) [5], Se speciation is dominated by selenate ($Se^{VI}O_4^{2-}$) or selenite ($Se^{IV}O_3^{2-}$) oxyanions, respectively [6]. Under these conditions Se species were found to be immobilized by cementitious materials [7,8]. For example, relatively high distribution ratios (R_d) for SeO_3^{2-} uptake by various cement formulations have been reported (0.25 $m^3\ kg^{-1} < R_d < 0.93\ m^3\ kg^{-1}$) by Johnson et al. [7], indicating significant interaction of the species with the cement matrix. Sorption

* Corresponding author. Tel.: +41 310 22 91; fax: +41 56 310 45 95.
E-mail address: erich.wieland@psi.ch (E. Wieland).

0008-8846/$ - see front matter © 2005 Elsevier Ltd. All rights reserved.
doi:10.1016/j.cemconres.2005.05.003

studies carried out on the cement minerals calcium silicate hydrate, ettringite, and monosulfate revealed a similar affinity of SeO_3^{2-} for all these phases ($0.18\ m^3\ kg^{-1} < R_d < 0.38\ m^3\ kg^{-1}$) [9]. In contrast, SeO_4^{2-} was found to sorb more strongly on monosulfate ($R_d \sim 2\ m^3\ kg^{-1}$) than on the other cement minerals and SeO_4^{2-}/SO_4^{2-} substitution was suggested to be the dominant uptake process [9]. At present, however, it still remains to be known how Se species are bound in the complex cement matrix. Spectroscopic investigations of SeO_3^{2-} and SeO_4^{2-} binding in the cementitious materials were expected to fill this existing gap in our knowledge.

X-ray absorption spectroscopy (XAS) has been proven useful in investigations of the oxidation states and binding mechanisms of metal cations and anions in cementitious systems [10–21]. For this reason it was anticipated that Se *K*-edge XAS will provide information about changes in the redox state of the SeO_3^{2-} and SeO_4^{2-} species upon uptake by hydrated cement and cement minerals and, further, yield details of the local coordination environment of these species in cementitious systems (neighboring atoms, coordination number, and bond distances). The present XAS study was performed to investigate binding mechanisms of SeO_3^{2-} and SeO_4^{2-} to hardened cement paste (HCP) and important cement minerals, such as calcium silicate hydrate (C–S–H), portlandite (CH), ettringite (AFt) and monosulfate (AFm).

2. Material and methods

2.1. Preparation of XAS samples and wet chemistry studies on HCP

Sample preparations and wet chemistry studies were carried in a glove box (N_2 atmosphere; CO_2, $O_2 \leq 2$ ppm; $T = 25 \pm 3$ °C). The experiments were performed under a N_2 atmosphere to avoid possible contamination caused by $CaCO_3$ precipitation. HCP was prepared from sulphate-resisting Portland cement as described earlier [22,23] and the C–S–H gel ($CaO:SiO_2$ (C:S) weight ratio = 1.0) employed in the experiment was synthesized using a standard procedure [24]. CH was used as received ($Ca(OH)_2$, Merck). AFt ($3CaO{\cdot}Al_2O_3{\cdot}3CaSO_4{\cdot}32H_2O$) and AFm ($3CaO{\cdot}Al_2O_3{\cdot}CaSO_4{\cdot}12H_2O$) preparations are reported in Baur and Johnson [9]. Prior to the experiments, HCP, CH and C–S–H were pre-equilibrated in an artificial cement pore water (ACW) at pH 13.3 in order to avoid interference of phase transformation reactions with the uptake process. ACW had the composition of a cement pore water corresponding to the initial stage of cement degradation (Table 1) [23]. AFt and AFm were suspended in pre-saturated solutions as described earlier [9].

$Se^{IV/VI}$ stock solutions were prepared by dissolving Na_2SeO_4 or $Na_2SeO_3{\cdot}5H_2O$ in ACW (HCP, C–S–H, CH) or in pre-saturated solutions (AFt, AFm). HCP, C–S–H and CH samples were prepared by mixing 1 g crushed HCP or CH, respectively, or 7 g wet C–S–H with 36 mL ACW. Se stock solutions at 4 mL aliquots were added to achieve an initial Se concentration of $5{\cdot}10^{-3}$ M in the suspensions. AFt and AFm samples were prepared by mixing 1 g dry material with pre-saturated solutions (AFt: 500 mL, AFm: 100 mL) and adding Se stock solutions ($[Se^{IV/VI}]_{tot} = 5{\cdot}10^{-3}$ and $5{\cdot}10^{-2}$ M). The suspensions were shaken end-over-end (HCP, C–S–H, CH: 60 days; AFt, AFm: 30 days) and centrifuged (60 min at 95,000×*g*). Aliquots of the supernatant solutions were analysed by ICP-AES (inductively coupled plasma-atomic emission spectrometry). The residual wet solids were sealed with Kapton tape in plexiglas holders and used for the XAS measurements. Details about the Se samples are given in Table 1. It is to be noted that a

Table 1
Chemical conditions of Se(IV/VI) sample preparation for XAS

Sample	Solid (g L^{-1})	Solution pH[a]	Curing[b] (days)	$[Se]_{tot}$ (mM)	$[Se]_{sorbed}$ (ppm)	Aging (days)
Se(IV)						
Se^{IV}–C–S–H[c]	17.5	13.3	6	5	1500	60
Se^{IV}–CH	25	13.3	3	5	2400	60
Se^{IV}–AFt	2	11.0	6	5	8800	30
Se^{IV}–AFm	10	11.7	6	10	5700	30
Se^{IV}–HCP	25	13.3	3	5	5000	60
Se(VI)						
Se^{VI}–C–S–H[c]	17.5	13.3	6	5	1200	60
Se^{VI}–CH	25	13.3	3	5	1600	60
Se^{VI}–AFt	2	11.0	6	5	3900	30
Se^{VI}–AFm	10	11.7	6	10	7300	30
Se^{VI}–HCP	25	13.3	3	5	2200	60

[a] C–S–H and CH were pre-equilibrated with ACW ($[Ca] = 1.6{\cdot}10^{-3}$ M, [Na] = 0.114 M, [K] = 0.18 M). For HCP, the chemical composition of ACW was complemented by adding Al(III) and SO_4^{2-} ($[Ca] = 1.6{\cdot}10^{-3}$ M, [Na] = 0.114 M, [K] = 0.18 M, $[Al] = 5{\cdot}10^{-5}$ M, $[S] = 2{\cdot}10^{-3}$ M). AFt and AFm were suspended in pre-saturated solutions [9].

[b] Curing refers to pre-equilibration of the solid in the corresponding solution.

[c] The water content was determined to be about 90 wt.% upon drying wet C–S–H at 100 °C until constant weight. C:S weight ratio = 1.0.

minimum Se loading of 1200 ppm was required to allow optimal measuring conditions.

XAS reference samples were prepared by diluting $CaSeO_3$ and $CaSeO_4 \cdot 2H_2O$ with cellulose. Synthesis of the solids is reported in Baur and Johnson [9]. Further, reference data were collected for Se(IV) and Se(VI) stock solutions in ACW (denoted as $Se^{IV}O_3^{2-}$ and $Se^{VI}O_4^{2-}$ reference samples).

Two sorption isotherms for Se(IV) and Se(VI) were determined on HCP in ACW (solid to liquid (S/L) ratio = $2.5 \cdot 10^{-2}$ kg L^{-1}, $5 \cdot 10^{-6}$ M < $[Se]_{tot}$ < 10^{-2} M) to assess the concentration range for linear sorption in these systems. The suspensions were shaken end-over-end for 15 days to reach equilibrium and centrifuged (60 min at 95,000 × g). Aliquots of the supernatant were analysed by ICP-AES. The partitioning of Se between solid and solution was quantified in terms of a distribution ratio (R_d value):

$$R_d = \frac{c_s}{c_{aq}} = \left(\frac{c_{tot} - c_{aq}}{c_{aq}}\right) \cdot \left(\frac{V}{m}\right) \quad [m^3 kg^{-1}] \qquad (1)$$

where c_s and c_{aq} denote Se concentrations measured on the solid [mol kg^{-1}] and in solution [mol L^{-1}], respectively, at equilibrium. The difference between total Se concentration added to the suspensions (c_{tot}) and the Se concentration of the supernatant solution after phase separation (c_{aq}) represents the Se concentration on the solid. V and m denote the volume of the suspension [m^3] and the mass of solid phase [kg], respectively.

2.2. Se K-edge (12.6 keV) X-ray absorption spectroscopy

The XAS measurements were conducted at the Swiss Norwegian Beam Line (SNBL) at the European Synchrotron Radiation Facility (ESRF), Grenoble, France, using a channel cut crystal monochromator (Si 111) in transmission (ionization chambers; I_0: 90% N_2/10% Ar; I_1: 70% N_2/30% Ar) and fluorescence modes (Lytle detector; 100% Kr; As-3 filter). A Se metallic foil was used for energy calibration. The measurements were performed at room temperature with the CO_2 sensitive samples placed inside an airtight box flushed with N_2.

Treatment of the extended X-ray absorption fine structure (EXAFS) data was conducted using the set of programs 'EXAFS pour le Mac' [25] and standard methods: pre-edge extrapolation by a linear function, atomic absorption removal using a sixth order polynomial function, normalization by the Heitler–Heisenberger method. The origin energy, E_0, was assigned to the maximum of the absorption edge. The pseudo radial distribution functions (PRDFs) were obtained by Fourier transformation of the k^3-weighted EXAFS oscillations (k-range: 2.5–14.2 $Å^{-1}$) using a Kaiser apodization window ($\tau = 3$). In the Se(VI)–HCP sample, a feature at ~10 Å was detected (see Fig. 4b), which is attributed to L_{III} Pb edge (13 035 eV) features caused by small amounts of Pb impurities in HCP (39 ppm). In order to avoid this contribution in the Se(VI)–HCP PRDF, it was necessary to perform the Fourier transformation (FT) in the 2.5–9.5 $Å^{-1}$ k-range, instead of the 2.5–14.2 $Å^{-1}$ k-range used for the other samples. As a consequence, the Se(VI)-PRDF has a lower resolution (broader peak in Fig. 4a).

Data fitting was performed using the 'Round Midnight' code and FEFF7 phases and amplitudes [25,26]. The fits included only single scattering features based on the assumption that linear chains of three or more atoms are unlikely in these systems, and thus, the multiple scattering paths are negligible. The reduction factor, S_0^2, and the mean free path, Γ ($= k/\lambda(k)$), were included in the fit as given by FEFF7. The shift between the E_0 value fixed in the experimental spectra and the E_0 value used by FEFF7 was determined from simulations of the EXAFS spectra for the reference compounds (Se^{IV}: $\Delta E_0 = 6.7$ eV; Se^{VI}: $\Delta E_0 = 5.3$ eV). For the sorption samples, ΔE_0 was bound by the values determined for reference compounds ($4 < \Delta E_0 < 8$ eV) and a unique energy threshold ΔE_0 was fitted for all shells of an adjustment. The fitted $k\chi(k)$ functions were obtained by inverse Fourier transformation (R range = 0.9–1.5 Å). To account for the low intensity of high-k EXAFS oscillations, fitting was conducted using the weighting function $w(k)$ ($w(k) = k^{2q}/A$; A: mean of the standard deviation pondered by q, which was set to 1.5). Floating parameters for the first peak analysis were the Debye–Waller factor, σ, and the Se–O distance, R. The statistical error bars on the fitted parameters were calculated using the procedure described earlier [27,28].

3. Results and discussion

3.1. Wet chemistry

Fig. 1 shows the Se(IV) and Se(VI) sorption isotherms for HCP. $CaSeO_3$ solubility limit is estimated at about $[Se^{IV}]_{aq} = 3 \cdot 10^{-3}$ M using reported thermodynamic data [9]. $CaSeO_4$ precipitation can be excluded in the concentration range $[Se^{VI}]_{aq} < 10^{-2}$ M. The sorption isotherms are of Freundlich type (slope <1) with R_d ranging in value between 0.02 m^3 kg^{-1} (high $[Se]_{tot}$ concentration range) and 0.2 m^3 kg^{-1} (dilute $[Se]_{tot}$ concentration range) for Se(IV) and between 0.002 m^3 kg^{-1} (high $[Se]_{tot}$) and 0.02 m^3 kg^{-1} (low $[Se]_{tot}$) for Se(VI).

The R_d values for Se(IV) are lower than those previously reported in Ref. [7] (0.57 m^3 $kg^{-1} < R_d < 0.93$ m^3 kg^{-1}). The discrepancy between the two sets of data is attributed to different procedures used for the preparation of the cement formulations (e.g., water to cement ratio (w/c) = 0.45–0.55 in Ref. [7] compared with $w/c = 1.3$ in this study) and differences in the experimental conditions (e.g., pH = 12.4 of an NaOH-containing wash solution [7] compared with pH = 13.3 of the ACW employed in this study). It is to be noted that $[Se]_{tot}$ was at maximum $1.9 \cdot 10^{-5}$ M in the study of Johnson et al. [7], whereas in this study, $[Se]_{tot}$ ranges in value between $5 \cdot 10^{-6}$ and 10^{-2} M. Interestingly, the

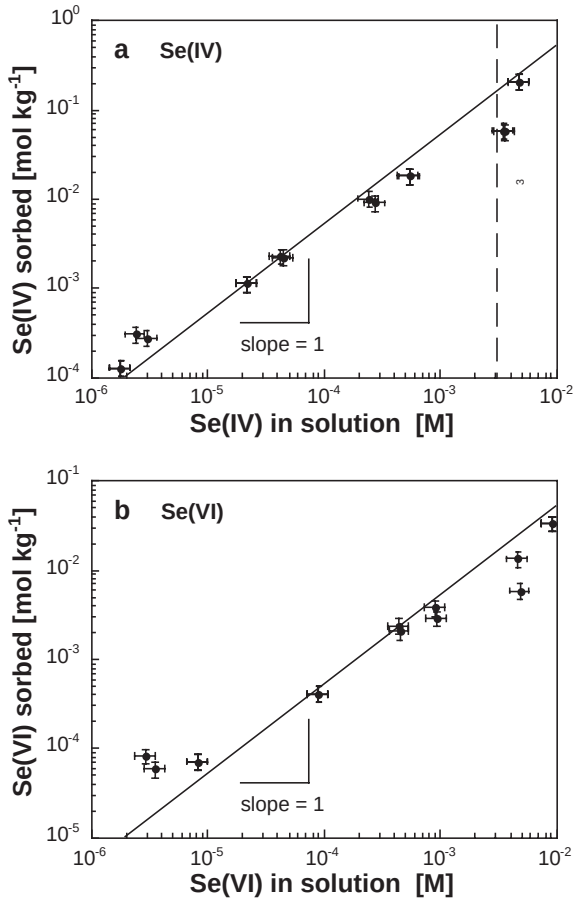

Fig. 1. [Se(IV)] (a) and [Se(VI)] (b) sorbed on HCP are shown as a function of $[Se]_{aq}$ after equilibration. Experimental conditions: HCP in ACW (S/L ratio = $2.5 \cdot 10^{-2}$ kg L^{-1}), $5 \cdot 10^{-6} < [Se]_{tot} < 10^{-2}$ M, equilibration time = 15 days. $CaSeO_3$ solubility was calculated using the thermodynamic data reported by Baur and Johnson [9]. Solubility and stability constants were adjusted for the ionic strength of the solution using the Davies equation.

discrepancy in the R_d values is less pronounced if data determined in the same Se(IV) concentration range are compared. R_d values differ by less than a factor of 4 at $[Se]_{tot} \leq 1.9 \cdot 10^{-5}$ M, which is expected to be the experimental uncertainty range in view of the different experimental protocols used in the two studies. Furthermore, Johnson et al. [7] observed linear sorption in the Se(IV) concentration range between $8 \cdot 10^{-8}$ and $5 \cdot 10^{-5}$ M. This suggests that, at low loadings, one specific type of site is available for Se(IV) binding to a specific cement mineral of the cement matrix.

Site saturation may cause deviation from linear sorption at increased Se(IV/VI) concentrations as observed in this study. The Freundlich type sorption behavior at high loadings implies Se(IV/VI) binding to various surface (or exchangeable) sites in terms of non-specific interactions with the cement matrix. The lower R_d value of Se(VI) compared with Se(IV) finally reflects the previously reported higher mobility of the SeO_4^{2-} anion [4]. From the above discussion it clearly emerges that a comparison of the sorption behavior of Se(IV/VI) in the different cement system, which is solely based on wet chemistry data, is speculative due to lack of knowledge on the sorption processes. This situation can only be improved by using spectroscopic techniques, which yield molecular-level information of the binding mechanisms of Se(IV/VI) oxyanions in the different cement matrices.

3.2. XANES

The X-ray absorption near edge structure (XANES) spectra for the HCP and reference samples are shown in Fig. 2. The XANES spectra are highly characteristic of the Se(IV) and Se(VI) oxidation states. A shift of ~3 eV is observed between the white lines (edge maximum) of the Se(IV) and Se(VI) species. The white line is followed by strong oscillations caused by the three or four oxygen, respectively, of the rigid SeO_3^{2-} and SeO_4^{2-} anions.

The typical XANES features of the $CaSeO_3$ and $CaSeO_4$ compounds (12,675–12,700 eV) do not appear in the spectra of the HCP samples (Fig. 2). This indicates the absence of $CaSeO_3$ and $CaSeO_4$ precipitates in the samples, corroborating the findings from the wet chemistry experiments (Fig. 1). Furthermore, the edge positions clearly correspond to the expected oxidation states, that is Se(IV) and Se(VI), suggesting that the oxidation states are stable under the given experimental conditions and that the SeO_3^{2-} and SeO_4^{2-} entities are preserved upon uptake by HCP. Thus, despite the negative potential determined in the suspensions during preparation of the Se(IV)- and Se(VI)-

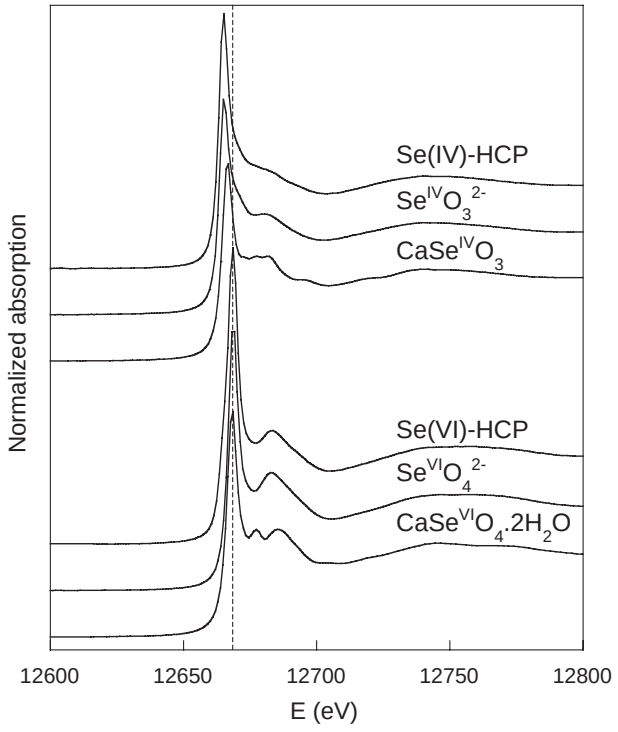

Fig. 2. Se *K*-edge XANES spectra of Se reference compounds ($Se^{IV}O_3^{2-}$ and $Se^{VI}O_4^{2-}$ solutions; $CaSe^{IV}O_3$(s) and $CaSe^{VI}O_4$(s)) and of Se immobilized by HCP (Se(IV)–HCP and Se(VI)–HCP).

treated cement samples (-300 mV$<E_h<-100$ mV) and the positive potential of the Se(VI)/Se(IV) redox couple ($E_h(Se^{VI}O_4^{2-}/Se^{IV}O_3^{2-})=+50$ mV) [29], no significant reduction of Se(VI) to Se(IV) was observed for time periods up to 60 days.

3.3. EXAFS of Se(IV) immobilization by HCP and cement minerals

Fig. 3a and b show the PRDF and the *k*-weighted EXAFS data of the Se(IV)-treated HCP and cement mineral samples and relevant reference compounds. All the spectra reveal a single oscillation with comparable frequency and amplitude, indicating similar coordination environments for Se(IV) in these samples. The PRDF for all the samples, i.e., the Se(IV) references (SeO_3^{2-}(aq), $CaSeO_3$) and the sorption samples (Se(IV)–HCP/C–S–H/CH/AFt/AFm), show a characteristic peak at 1.3 Å (not corrected for phase shift) (Fig. 3a). Peaks at longer distance appear in the $CaSeO_3$ PRDF (*R* range between 2.5 and 4.5 Å). In contrast, the PRDF for all sorption samples are similar to that of the SeO_3^{2-} in solution and shows no further peak above the noise level (Fig. 3a).

Since the FT spectra show no further PRDF peaks at longer distance, the structural information obtained from EXAFS data analysis is limited to the first coordination shell. It is further assumed that the triangular coordination of Se(IV) with oxygen remained intact upon uptake of the anion by the cement matrix and cement minerals. This assumption is supported by the XANES (Fig. 2) and the fact that the EXAFS spectra of the sorption samples and the aqueous SeO_3^{2-} species reveal a single oscillation with the same frequency and amplitude (Fig. 3b). For this reason, the number of oxygen first neighbors was fixed at 3 in the fitting and only one Se–O shell was considered. The goodness of fits (2.9%<rf<4.8%) further supported this approach (Table 2). Se–O distances deduced from data analysis are found to be identical for all the samples (1.70 Å) within the experimental error (±0.01 Å). Furthermore, the Se–O distance deduced in this study agrees with literature data [30].

The absence of any contributions from second neighbors indicates that SeO_3^{2-} is bound in a "solution-like" chemical environment by the cement matrix and the cement minerals. This finding further suggests that non-specific interaction with the surface of C–S–H, CH, AFt, and AFm occurs or SeO_3^{2-} incorporation into the structure of the cement minerals, e.g., AFt and AFm, takes place without any direct bonding to neighboring atoms at distances shorter than ~3.5 Å. The absence of any significant backscattering contributions from atoms at short distance in the cementitious systems is noteworthy because direct bonding of Se(IV) has previously been reported on iron and manganese oxides (inner-sphere surface complexation) in the near neutral pH range (5–8) and similar surface loadings (600–10,000 ppm) [31,32]. In these studies SeO_3^{2-} was found to form bidentate mononuclear (edge-sharing) or monodentate mononuclear (corner-sharing) complexes with the Fe and Mn surface sites. The bond distances between Se and the second shell atoms, i.e., Se–Fe and Se–Mn bond lengths, were determined to be 3.38 [31] and 3.07–3.49 Å [32], respectively, depending on the structural arrangement of Se(IV) on the solid surface. For the cementitious systems investigated in this study, wet

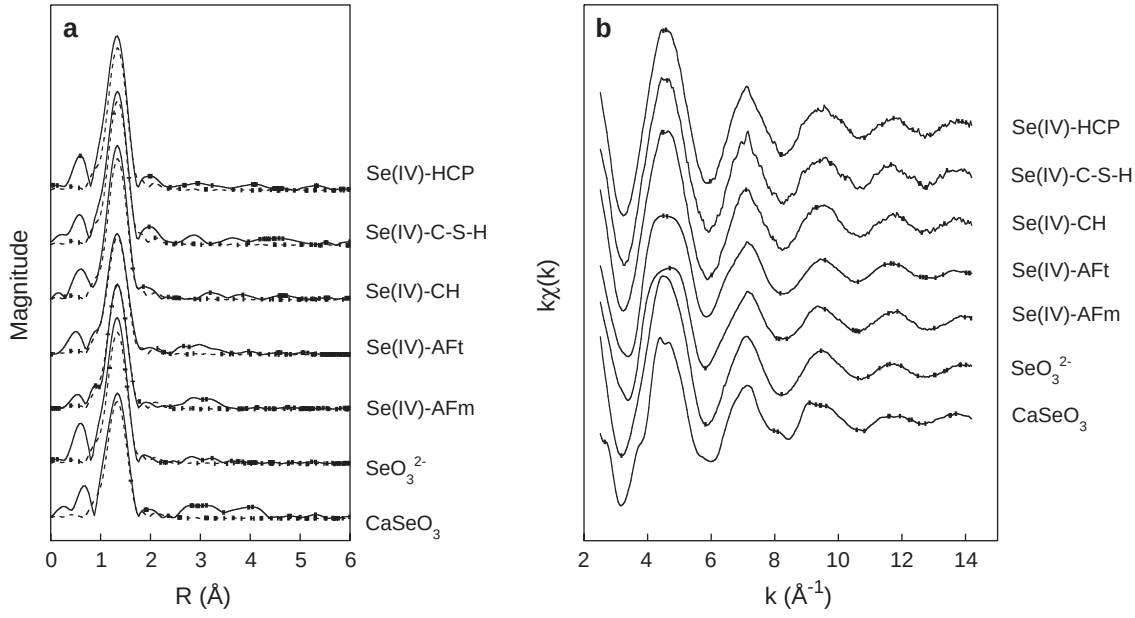

Fig. 3. a. Experimental Se *K*-edge PRDF modulus (—) for Se(IV) bound to solid materials (HCP, C–S–H, CH, AFt, and AFm) and for the Se(IV) reference compounds ($Se^{IV}O_3^{2-}$ solution and $CaSe^{IV}O_3$(s)) compared with simulated modulus (---) (see Table 2 for fitting results). b. Corresponding experimental Se *K*-edge EXAFS oscillations.

Table 2
Coordination numbers (N), interatomic distance (R), Debye–Waller factor (σ^2) and inner potential correction (ΔE_0) as obtained from EXAFS Se K-edge data analysis

Sample	Shell	N[a]	R [Å]	σ^2 10^{-3} [Å^2]	ΔE_0 [eV]	rf[b]
References						
$CaSe^{IV}O_3$	Se–O	3	1.70±0.01	1.8±0.1	6.7	3.1
$Se^{IV}O_3^{2-}$	Se–O	3	1.70±0.01	1.4±0.2	6.7	3.3
$CaSe^{VI}O_4$	Se–O	4	1.64±0.01	4.2±0.5	5.3	2.6
$Se^{VI}O_4^{2-}$	Se–O	4	1.64±0.01	3.4±0.7	5.3	6.9
Se(IV) sorption samples						
Se^{IV}–HCP	Se–O	3	1.70±0.01	1.0±0.3	6.7	4.0
Se^{IV}–C–S–H	Se–O	3	1.70±0.02	1.6±0.8	6.9	2.9
Se^{IV}–CH	Se–O	3	1.70±0.01	1.0±0.3	7.0	3.3
Se^{IV}–AFt	Se–O	3	1.70±0.01	2.2±0.4	7.0	4.8
Se^{IV}–AFm	Se–O	3	1.70±0.01	1.8±0.4	7.0	4.4
Se(VI) sorption samples						
Se^{VI}–HCP	Se–O	4	1.65±0.04	1.0±0.5	5.0	6.2
Se^{VI}–C–S–H	Se–O	4	1.65±0.01	1.3±0.3	7.1	1.7
Se^{VI}–CH	Se–O	4	1.65±0.02	1.0±0.7	7.1	7.4
Se^{VI}–AFt	Se–O	4	1.65±0.01	1.0±0.3	5.7	2.1
Se^{VI}–AFm	Se–O	4	1.65±0.01	1.7±0.4	7.1	3.5

[a] Value held fixed during the fitting procedure.
[b] Residual factor $\left(rf = \frac{\sum_{i=1}^{n}[k\chi\exp - k\chi theo]^2}{\sum_{i=1}^{n}[k\chi\exp]^2}100\right)$ represents the quality of the fit (%).

chemistry experiments indicate a significant interaction of Se(IV) with the cement matrix and cement minerals, which, according to the EXAFS results, cannot be attributed to the specific binding of Se(IV) to cement minerals. One may speculate that a significant degree of disorder in the population of the second shell atoms (Ca, Al, Si) in these minerals gives rise to destructive interference of the single scattering paths and therefore an apparent reduction in backscattering. Nevertheless, it should be noted that non-specific binding of Se(IV) to cement minerals was previously suggested by Baur and Johnson [9] based on sorption experiments. The authors found that SeO_3^{2-} did not bind preferentially to any of the important cement minerals, i.e., AFt, AFm and C–S–H, at Se(IV) loadings similar to those used in the present study.

3.4. EXAFS of Se(VI) immobilization by HCP and cement minerals

Fig. 4a and b show the PRDF and the k-weighted EXAFS data of the Se(VI)-treated HCP and cement mineral samples and relevant reference compounds. The spectra reveal features already found in the Se(IV) samples, i.e., a single oscillation with comparable frequency and amplitude, indicating similar coordination environments for Se(VI) in all the samples. The EXAFS spectra of the sorption samples and the aqueous SeO_4^{2-} species are identical. Nevertheless, the spectra are very different from the one of $CaSeO_4$ (Fig. 4b). Note that the low signal/noise ratio in the EXAFS spectra of the Se(VI)–C–S–H/CH samples is caused by the low Se(VI) loadings.

As in the case of Se(IV), the structural information obtained from EXAFS data analysis is limited to the first coordination shell because the FT show no further PRDF peaks at longer distance. Furthermore, it is assumed that the SeO_4^{2-} structural entity remained upon uptake of the anion by HCP, C–S–H, CH, AFt and AFm. This assumption is

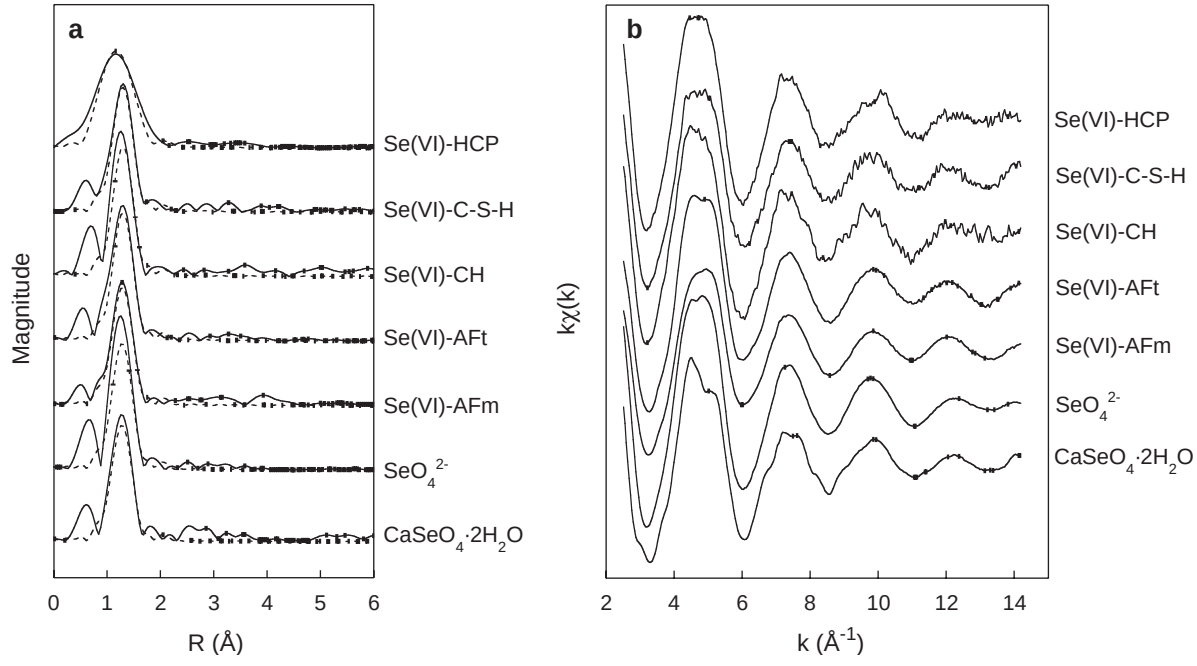

Fig. 4. a. Se K-edge PRDF for Se(VI) bound to solid materials (HCP, C–S–H, CH, AFt, AFm) and for the Se(VI) reference compounds ($Se^{VI}O_4^{2-}$ solution and $CaSe^{VI}O_4$(s)) compared with simulated modulus (---) (see Table 2 for fitting results). b. Corresponding experimental Se K-edge EXAFS oscillations.

supported by XANES (Fig. 2) and the goodness of the fit results (Table 2). The Se–O distances determined from the EXAFS data are found to be identical for all the samples (1.64 Å) within the experimental error (±0.01 Å). As in the case of Se(IV), this finding suggests a "solution-like" coordination environment for SeO_4^{2-} bound in the cement matrix and further implies non-specific interaction with the surface sites of the cement minerals or SeO_4^{2-} incorporation into the structure of the cement minerals with no specific bonding to neighboring atoms. Interestingly, the non-specific interactions give rise to small but measurable uptake of SeO_4^{2-} by the cement matrix and cement minerals as observed from the wet chemistry experiments in this and a previous study [9]. It should be noted that, as in the case of Se(IV), EXAFS has indicated SeO_4^{2-} binding to surface sites of iron oxyhydroxides either as outer-sphere [31,34] or inner-sphere complexes [33,34]. Therefore, the absence of backscattering atoms in the cementitious systems within the distance probed by EXAFS (~5 Å) was not anticipated in view of these earlier studies.

The first peak in the Se(VI)-AFm PRDF appears to be lower than in the spectra of the other sorption samples (Fig. 4a). The corresponding fit gives rise to a higher Debye–Waller factor (Table 2), which may indicate a larger distribution of Se–O distances upon uptake by AFm. Nevertheless, the results show that the chemical environment of SeO_4^{2-} is "solution-like" in AFm within the ~5 Å distance probed by EXAFS. Substitution of SO_4^{2-} by SeO_4^{2-} in AFm was recently proposed to be the main binding mechanism of Se(VI) in cement systems [9]. SO_4^{2-} is expected to be bound in the AFm interlayers in between hexagonal lamellar platelets together with neighboring water molecules [35]. The results of this study are in agreement with a model based on the replacement of SO_4^{2-} by SeO_4^{2-}, which would imply that water molecules are the only nearest neighboring species.

4. Conclusion

In this study we demonstrate that Se *K*-edge XAS is capable of yielding information about SeO_3^{2-} and SeO_4^{2-} speciation in cementitious materials. Redox reactions do not influence uptake processes in the cementitious systems as both Se(IV) and Se(VI) oxidation states are found to be stable under the given experimental conditions for time periods up to 60 days. The SeO_3^{2-} and SeO_4^{2-} structural entities undergo no modification upon uptake by HCP and the cement minerals AFt, AFm, CH and C–S–H. The spectra for the SeO_3^{2-} and SeO_4^{2-}-treated HCP and cement mineral samples reveal a chemical environment of the sorbed species similar to those of the aqueous SeO_3^{2-} and SeO_4^{2-} species ("solution-like" chemical environment). The absence of backscattering atoms within the distance probed by EXAFS suggests: (1) non-specific interaction of the SeO_3^{2-} and SeO_4^{2-} species with the surface of the cement minerals or (2) incorporation of these anions into the structure of the minerals with no direct bonding to neighboring atoms, presumably into channels and interlayers in the lattice of these phases.

Acknowledgments

Experimental assistance from the staff of the Swiss–Norwegian Beam Line (SNBL) at the ESRF is gratefully acknowledged. The authors wish to thank Jan Tits (PSI) for assistance with the C–S–H preparation. Thanks are extended to M. Bradbury (PSI) and R. Dähn (PSI) for the many helpful discussions and comments on the manuscript. The authors gratefully acknowledge the funding of the Swiss Federal Institute of Environmental Science and Technology (EAWAG). Partial financial support was provided by the National Cooperative for the Disposal of Radioactive Waste (Nagra), Switzerland.

References

[1] P.H. Masscheleyn, R.D. Delaune, W.H. Patrick, Arsenic and selenium chemistry as affected by sediment redox potential and pH, J. Environ. Qual. 20 (1991) 522–527.
[2] G.B. Dreher, R.B. Finkelman, Selenium mobilization in a surface coal-mine, powder river basin, Wyoming, USA, Environ. Geol. Water Sci. 19 (1992) 155–167.
[3] A.J. Chandler, T.T. Eighmy, J. Hartlén, O. Hjelmar, D.S. Kosson, S.E. Sawell, H.A. Van der Sloot, J. Vehlow, Municipal solid waste incinerator residues/The international ash working group, Studies in Environmental Sciences, vol. 67, Elsevier, Amsterdam, 1997.
[4] F. Chen, P.C. Burns, R.C. Ewing, ^{79}Se: geochemical and crystallo-chemical retardation mechanisms, J. Nucl. Mater. 275 (1999) 81–94.
[5] U.R. Berner. (1999) PSI Report 99-10. Villigen, Switzerland.
[6] D.G. Brookins, Eh–pH Diagrams for Geochemistry, Springer-Verlag, Berlin, 1988.
[7] E.A. Johnson, M.J. Rudin, S.M. Steinberg, W.H. Johnson, The sorption of selenite on various cement formulations, Waste Manage. 20 (2000) 509–516.
[8] D. Sugiyama, T. Fujita, Sorption of radionuclides onto cement materials altered by hydrothermal reaction, Mater. Res. Soc. Symp. Proc. 556 (1999) 1123–1130.
[9] I. Baur, C.A. Johnson, Sorption of selenite and selenate to cement minerals, Environ. Sci. Technol. 37 (2003) 3442–3447.
[10] P.G. Allen, G.S. Siemering, D.K. Shuh, J.J. Bucher, N.M. Edelstein, C.A. Langton, S.B. Clark, T. Reich, M.A. Denecke, Technetium speciation in cement waste forms determined by X-ray absorption fine structure spectroscopy, Radiochim. Acta 76 (1997) 77–86.
[11] I. Bonhoure, A.M. Scheidegger, E. Wieland, R. Dähn, Iodine species uptake by cement and CSH studied by I *K*-edge absorption spectroscopy, Radiochim. Acta 90 (9–11) (2002) 647–651.
[12] I. Bonhoure, E. Wieland, A.M. Scheidegger, M. Ochs, D. Kunz, EXAFS study of Sn(IV) immobilization by hardened cement paste and calcium silicate hydrates, Environ. Sci. Technol. 37 (10) (2003) 2184–2191.
[13] M.-P. Pomiés, N. Lequeux, P. Boch, Speciation of cadmium in cement: Part I. Cd^{2+} uptake by CSH, Cem. Concr. Res. 31 (2001) 563–569.
[14] M.-P. Pomiés, N. Lequeux, P. Boch, Speciation of cadmium in cement: Part II. C_3S hydration with Cd^{2+} solution, Cem. Concr. Res. 31 (2001) 571–576.

[15] J. Rose, I. Moulin, J.-L. Hazemann, A. Masion, P.M. Bertsch, J.-Y. Bottero, F. Mosnier, C. Haehnel, X-ray absorption spectroscopy study of immobilization processes for heavy metals in calcium silicate hydrates: 1. Case of lead, Langmuir 16 (2000) 9900–9906.
[16] J. Rose, I. Moulin, A. Masion, P.M. Bertsch, M.R. Wiesner, J.-Y. Bottero, F. Mosnier, C. Haehnel, X-ray absorption spectroscopy study of immobilization processes for heavy metals in calcium silicate hydrates: 2. Zinc, Langmuir 17 (2001) 3658–3665.
[17] A.M. Scheidegger, E. Wieland, A.C. Scheinost, R. Dähn, P. Spieler, Spectroscopic evidence for the formation of layered Ni–Al double hydroxides in cement, Environ. Sci. Technol. 34 (2000) 4545–4548.
[18] A.M. Scheidegger, E. Wieland, A.C. Scheinost, R. Dähn, J. Tits, P. Spieler, Ni phases formed in cement and cement systems under highly alkaline conditions: an XAFS study, J. Synchrotron Radiat. 8 (2001) 916–918.
[19] C.E. Tommaseo, M. Kersten, Aqueous solubility diagrams for cementitious waste stabilization systems: 3. Mechanism of zinc immobilization by calcium silicate hydrate, Environ. Sci. Technol. 36 (2002) 2919–2925.
[20] B.E. Viani, P. Zhao, P.G. Allen, E.R. Sylwester, The partitioning of uranium and neptunium onto hydrothermally altered concrete, Radiochim. Acta 88 (2000) 729–736.
[21] F. Ziegler, A.M. Scheidegger, A.C. Johnson, R. Dähn, E. Wieland, Sorption mechanisms of zinc to calcium silicate hydrate: X-ray absorption fine structure (XAFS) investigation, Environ. Sci. Technol. 35 (2001) 1550–1555.
[22] F.-A. Sarrot, M.H. Bradbury, P. Pandolfo, P. Spieler, Diffusion and adsorption studies on hardened cement paste and the effect of carbonation on diffusion rates, Cem. Concr. Res. 22 (1992) 439–444.
[23] J. Tits, A. Jakob, E. Wieland, P. Spieler, Diffusion of tritiated water and Na-22 through non-degraded hardened cement pastes, J. Contam. Hydrol. 61 (1–4) (2003) 45–62.
[24] M. Atkins, F.P. Glasser, A Kindness. (1991) DoE report DoE/HMIP/RR/92/005.
[25] A. Michalowicz, "EXAFS pour le Mac": a new version of an EXAFS data analysis code for the Macintosh, J. Phys., IV 7 (1997) C 2–C 235.
[26] A.L. Ankudinov, J.J. Rehr, Relativistic calculations of spin-dependant X-ray absorption spectra, J. Phys. Rev., B 56 (1997) 1712–1721.
[27] I. Bonhoure, C. Den Auwer, C. Cartier dit Moulin, P. Moisy, J.-C. Berthet, C. Madic, Molecular and electronic structure of AnIV-FeII(CN)6. × H_2O (An=Th, U, Np) compounds: an X-ray absorption spectroscopy investigation, Can. J. Chem. 78 (2000) 1305–1317.
[28] Error reporting recommendations: a report of the standards and criteria committee, IXS Standards and Criteria Subcommittee. http://ixs.csrri.iit.edu/IXS/subcommittee_reports/sc/ (accessed Jul 2002).
[29] R.D. Lide, CRC Handbook of Chemistry and Physics, 83rd ed., CRC Press, LLC, Boca Raton, 2002.
[30] A. Manceau, D.L. Gallup, Removal of selenocyanate in water by precipitation: characterization of copper–selenium precipitate by X-ray diffraction, infrared, and X-ray absorption spectroscopy, Environ. Sci. Technol. 31 (1997) 968–976.
[31] K.F. Hayes, A.L. Roe, G.E. Brown, K.O. Hodgson, J.O. Leckie, G.A. Parks, In situ x-ray absorption study of surface complexes: selenium oxoanions on α-FeOOH, Science 238 (1987) 783–786.
[32] A.L. Foster, G.E. Brown, G.A. Parks, X-ray absorption fine structure study of As(V) and Se(IV) sorption complexes on hydrous Mn oxides, Geochim. Cosmochim. Acta 67 (2003) 1937–1953.
[33] A. Manceau, L. Charlet, The mechanism of selenate adsorption on goethite and hydrous ferric oxides, J. Colloid Interface Sci. 168 (1994) 87–93.
[34] D. Peak, D.L. Sparks, Mechanisms of selenate adsorption on iron oxides and hydroxides, Environ. Sci. Technol. 36 (2002) 1460–1466.
[35] H.F.W. Taylor, Cement Chemistry, 2nd ed., Thomas Telford, New York, 1997.